Available online at www.sciencedirect.com

SciVerse ScienceDirect

Ceramics International 38 (2012) 1755–1763

CERAMICS INTERNATIONAL

www.elsevier.com/locate/ceramint

Review paper

Effect of high alumina cement on permeability and structure properties of ZrO_2 composites

Y.L. Bruni [b], L.B. Garrido [a], E.F. Aglietti [b,*]

[a] CETMIC (Centro de Tecnología de Recursos Minerales y Cerámica, CIC-CONICET La Plata), Camino Centenario y 506, C.C.49 (B1897ZCA) M.B. Gonnet, Buenos Aires, Argentina

[b] Facultad de Ciencias Exactas de la Universidad Nacional de La Plata, Camino Centenario y 506, C.C.49 (B1897ZCA) M.B. Gonnet, Buenos Aires, Argentina

Received 23 September 2011; received in revised form 12 October 2011; accepted 13 October 2011
Available online 18 October 2011

Abstract

Porous ZrO_2 based ceramics are widely used for filtration/separation processes due to the good chemical and thermal stability. For these applications it is desirable that the material have a controlled porous structure in order to obtain good permeability. In this study Ca stabilized ZrO_2 composites were developed from a starting mixture of pure ZrO_2 containing different mole proportions of calcium aluminate cement. Ceramics disks were uniaxially pressed and subsequently sintered at 1300–1450 °C. The influence of process parameters such as chemical compositions and sintering temperature on textural characteristics (volume fraction of pores, pore size distribution) and permeability was followed by apparent density measurements, Hg porosimetry and N_2 permeation, respectively. Sintered microstructure was examined by scanning electron microscopy SEM. The XRD analysis showed that m-ZrO_2 transformed to tetragonal and/or cubic ZrO_2, these phases probably coexisted at relatively low CaO addition. For 30 mol% addition, amount of the cubic $Ca_{0.15}Zr_{0.85}O_{1.85}$ phase appreciably increased. At 50 mol% CaO, CA_2 was the major phase of the composite with minor $CaZrO_3$ formation whereas relative content c-ZrO_2 is slightly reduced.

The composites had 30–40 vol% porosity with typical pore radius of 1–1.3 μm and the corresponding Darcian permeability k_1 values varied between 2 and 4×10^{-14} m^2, such structure parameters slightly increased for high cement addition. The k_1 of ceramics produced from 50 mol% CaO composition remained nearly constant up to 1450 °C due to similar densification degree. The experimental permeability dependence on pore structure parameters as well as the comparison with the value estimated by Ergun's equation are showed.

Keywords: Porous zirconia; Aluminous cement; Structure properties; Permeability

Contents

* Corresponding author.
E-mail address: aglietti@cetmic.unlp.edu.ar (E.F. Aglietti).

0272-8842/$36.00 © 2011 Published by Elsevier Ltd and Techna Group S.r.l.
doi:10.1016/j.ceramint.2011.10.030

1. Introduction

Zirconia (ZrO_2) is a suitable material for the manufacture of a variety of porous ceramics with potential in engineering applications including sensors, filters for liquids and gases, catalyst supports for reactions, structural lightweight components, etc. [1–4]. The zirconia based ceramics shows a combination of excellent surface properties with good mechanical and chemical resistances and high thermal stability [5,6]. In particular, Ca stabilized ZrO_2 was recently proposed as a valuable material for bioceramics and for thermal insulation as this porous material exhibits good resistance for high temperature conditions due to a relatively low expansion coefficient [7,8].

In the field of filtration and separation processes and dust gas pollutants is also extensively studied. The development is directed to improving their technology [9,10] for porous ZrO_2 as membrane support and biomaterial.

Calcium aluminate cements (HAC) are employed in the refractory industry. Commercial HAC are pure materials of high melting point, which contains calcium aluminate (CA and CA_2) as principal crystalline phases accompanied by low contents of α-Al_2O_3 and $C_{12}A_7$. Reaction of HAC with zirconia at high temperatures delay in phases of the ZrO_2–CaO–Al_2O_3 system. Also HAC presents a relative low particle size that allows to be sintered or reacted with other compounds, in this case with zirconia [11].

Permeability is an important parameter determining of the multifunctional character of filters [12–16], this value can be controlled and improved during the processing of the ceramic product by adjusting properties such as pore volume and morphology, size and pore interconnection. Permeability optimization throughout process parameters can be achieved in order to reduce the pressure drop due to the fluid flow across the porous material.

The Forchheimer's equation and Darcy's Law (Eqs. (1) and (2), respectively) are widely used to evaluate the permeability coefficient considering the laminar flow of compressible fluids through a porous granular media [12–16]. The pressure drop due to the gas flow through a porous material is usually calculated according to the following equations:

$$\frac{P_1^2 - P_2^2}{2P_2L} = \frac{\mu}{k_1} v_s + \frac{\rho}{k_2} v_s^2 \quad (1)$$

$$\frac{P_1^2 - P_2^2}{2P_2L} = \frac{\mu}{k_1} v_s \quad (2)$$

where the pressure drop for compressible gas (Pa) is given as $(P_1^2 - P_2^2)/2P_2$, P_1 and P_2 are, respectively, the absolute values pressure measured at the inlet and outlet of the porous medium [Pa], respectively; v_s the gas velocity (m s^{-1}) calculated as the ratio between volume flow [m^3/s] and the cross section area [m^2] through the flow, μ the viscosity (Pa s), k_1 the permeability (m^2), L the thickness (m), k_2 the inertial permeability (m), ρ the gas density (kg m^{-3}).

Thus, experimental Darcian (k_1) and non-Darcian (k_2) permeability constants are determined by fitting of Forchheimer's equation to experimental pressure drop vs. gas velocity data. The k_1 and k_2 constants are considered mainly dependent on the porous structure of the material.

For cellular ceramics the application of Forchheimer's equation and validation of the Darcy's law to evaluate the permeability constants was extensively studied by Innocentini et al. [15,16]. More recently, investigations on ceramic foams verified that their permeability k_1 and k_2 may be also assessed using Eq. (1). Such constants are related to pore size and porosity [17–19]. For example, high porosity foams of hydroxyapatite with mean cell sizes of 517–603 μm show high permeability values varying between 0.40–3.24×10^{-9} m^2 and 3–175×10^{-6} m, respectively [18]. Contrarily, zirconia membranes with pores in the submicrometer range exhibited air permeability values as low as 1.5×10^{-19} m^2 [6].

On the other hand, a theoretical estimation of permeability constant k_1 from porous structure parameters can be made by following the well known Ergun's equation [20]. The prediction of the permeability is deduced by assuming a porous granular media formed by a non consolidated packed bed of spherical particles of identical size. Thus, k_1 is given by

$$k_1 = \frac{\varepsilon^3 d_p^2}{150(1-\varepsilon)^2} \quad (3)$$

where ε is the porosity (pore volume fraction), d_p is the equivalent diameter of particle of the porous media [m].

The particle diameter can be estimated from the definition of hydraulic radius for spherical particles making the porous media:

$$d_p = 1.5 \frac{(1-\varepsilon)}{\varepsilon} d_c \quad (4)$$

where d_c [m] is the average pore diameter of the structure.

Combining Eqs. (3) and (4), the evaluation of k_1 can be made considering that porous structure can be represented by two parameters such as the pore volume and the mean pore size or certain characteristic length. However, exists a somewhat variety of definitions of the characteristic length. As Ergun's equation requires the estimation of the characteristic length, the permeability prediction by application of this model is complex and should be validated with the experimental data. In particular, the theoretical permeability k_1 may be obtained

by means of the mean pore diameter measured by mercury porosimetry as an approximation to the pore size d_c.

In the present work, porous composites containing Ca stabilized ZrO_2 was developed by reactive sintering of a mixture of pure ZrO_2 and high alumina cement containing 30 wt% CaO. The stabilization of the zirconia phase was achieved through the addition of CaO, since the use of pure zirconia in applications that require high temperatures is limited due to the volumetric change that experiences during the cooling associated with m–t transformation (3–5%) and that causes the material failure.

One of the advantages of this fabrication method is the relatively low cost of the commercially available starting material used.

The influence of different initial compositions and sintering temperatures on textural properties and N_2 permeability was examined. N_2 permeability of the ceramics was experimentally measured from pressure drop vs. velocity curves and evaluated with the Forchheimer's equation. The deviation between such permeability constants and that evaluated using Darcy's equation was also calculated. A comparison between the experimental and predicted permeability provided by the Ergun's equation is also presented.

2. Experimental

2.1. Materials and preparation of ceramic disks

A commercially available pure zirconia powder with monoclinic phase structure (m-ZrO_2) was used. The particle size distribution of the zirconia powder exhibits a monomodal distribution with a mean particle diameter of 8 μm and contains less than 5 wt% of diameter finer than 1 μm. A 10 wt% fraction of the sample corresponds to coarser particles between 15 and 20 μm. SEM micrographs showed that zirconia powder consists of irregular aggregates which are formed of primary very fine crystallites with nearly spherical shape. The aggregated had a size similar to the mean size of the distribution.

The calcium aluminate cement used is commercially known as SECAR71, the main constituents are Al_2O_3 and CaO, its approximate chemical composition which was obtained from the product data sheet (KERNEOS, Inc.) is shown in Table 1.

The principal mineralogical phases are monocalcium aluminate CA and calcium dialuminate CA_2 and minor α-Al_2O_3. Main physical properties: specific gravity: 2.9–3.05 g/cm^3, residue at 90 μm: <5%. The pyrometric cone equivalent (on neat cement paste): 19–20 or approx. 1563 °C (2845 °F) and therefore, can be used at high temperatures up to 1400 °C.

From these two raw materials, a series of mixtures of different chemical composition was prepared by addition of 5–50 mol% of CaO in ZrO_2.

The ceramic mixture was formed using uniaxial dry pressing technique in compacts with a shape of disks of 30 mm in diameter and 5 mm in thickness and then dried at 100 °C. Finally, the disks were sintered at different sintering temperatures of 1300, 1400 and 1450 °C – 2 h in a furnace at a heating/cooling rate of 5 °C/min.

2.2. *X-ray diffraction analysis* ***XRD***

X-ray diffraction analysis (XRD) was carried out using a Philips diffractometer model PW3020 with radiation Cu-Kα and Ni filter in the region $2\theta = 10–80^\circ$. The relative proportion of m-ZrO_2 phase was determined semi quantitatively from the XRD diagrams using the method of Garvie and Nicholson [21] for mixtures of stabilized zirconia and monoclinic. This method allows to estimation of the fraction of m-ZrO_2 phase from the integrated peak areas representing the monoclinic and stabilized phases.

2.3. Textural characteristics: total porosity, Hg porosimetry

The textural properties such as porosity and pore size distribution are important factors that govern the material transport properties and depend on processing factors, and therefore were determined for the different ZrO_2 ceramics.

The total porosity of the sintered disks was calculated from relative density values, for which apparent density was geometrically determined; theoretical density of composite was estimated from the final phase composition obtained by DRX analysis and each phase density.

Pore volume and the most frequent pore radius of the ZrO_2 composites sintered at different temperatures were carried out in the Hg porosimeter Carlo Erba 2000 (Italy).

2.4. N_2 permeability

The characterization of N_2 permeability of disks produced from the various compositions and sintered at 1300, 1400 and 1450 °C was carried out at room temperature by passing the gas through the porous ceramic in an apparatus previously described [22]. The drop pressure across the ceramic was measured as a function of gas flow through it, being the sectional cross area and the thickness of the specimen in the flow direction known quantities.

The experimental pressure drop and volume flow data were first analyzed according to Forchheimer's law (Eq. (1)). Therefore, the Forchheimer's number F_0 and thus the error (F_0/

Table 1
Chemical composition of high alumina cement used.

HAC	Al_2O_3 (%)	CaO (%)	Na_2O (%)	SiO_2 (%)	Fe_2O_3 (%)	TiO_2 (%)
	68	30	0.5	0.2–0.6	0.1–0.2	0–0.4

$1 - F_0$) due to neglecting the non linear effects were calculated with the following expressions:

$$F_0 = \frac{\rho v_s}{\mu}\left(\frac{k_1}{k_2}\right) \quad (5)$$

$$\text{Error } (\%) = 100\frac{F_0}{F_0 + 1} \quad (6)$$

2.5. Microstructure characterization

The microstructure of the sintered samples was examined on fracture surfaces and polished surfaces (up to 1 μm) with a scanning electron microscope SEM (Quanta 200 FEI Series MK2) with X-ray energy dispersion spectrometer (EDS) on the polished surface.

3. Results and discussion

3.1. Crystalline phase composition of the ceramics sintered at 1400 °C

Fig. 1 shows the XRD patterns of samples produced from starting mixtures containing 5–50 mol% CaO in ZrO_2 and sintered at 1400 °C. The XRD analysis indicated that the sintered products prepared from the composition with 5–15% molar CaO were composed of the phases of zirconia: mainly monoclinic (m-ZrO_2) and stabilized (t-/c-ZrO_2). Also existed a minor amount of the calcium dialuminate ($CaAl_4O_7$) which is referred in the literature as CA_2. CA_2 is a phase constituent of the high alumina cement having a composition 21.7 wt% CaO and 78.3 wt% Al_2O_3 with characteristics reflections 2θ at 25.5°, 29°, 32.6° and 33.15°.

The diffusion of calcium from CaO phases of high alumina cement promoted the m → c-ZrO_2 phase transformation with stabilization of a Ca solid solution ($Ca_{0.15}Zr_{0.85}O_{1.85}$). However in such samples the stabilization of the cubic phase was partial and the monoclinic phase predominated.

In the sample with 30 mol% CaO, CA_2 appreciably increased, the relative content of Ca stabilized ZrO_2 was higher than that for 15 mol% addition due to the higher content of cement and hence of CaO in the starting composition. In this case, m-ZrO_2 consequently reduced and scarce $CaZrO_3$ was also identified.

For the composite with 50 mol% CaO, CA_2 was the major phase. The transformation of m-ZrO_2 to c-ZrO_2 phase was nearly complete. Simultaneously a relative reduction of c-ZrO_2 occurred as the content of $CaZrO_3$ slightly increased. Traces of unreacted α-Al_2O_3 were detected. The relative content of c-ZrO_2 remained nearly constant in a range of sintering temperatures between 1300 and 1450 °C.

The phase relations determined by XRD agreed well with the phase composition estimated according to chemical composition of the various samples from the ternary phase diagram for the system ZrO_2–CaO–Al_2O_3 at 1380 °C [23].

Moreover, reaction, phase transformation and sintering in the composition range above 30 mol% CaO probably evolved the presence of a liquid phase [24] which was favored by the concentration of impurities in the raw materials of less than 2 wt% of Fe_2O_3, SiO_2, TiO_2 (Table 1). Reactive sintering of the other samples occurred as a solid state process.

Fig. 2 shows that the relative proportion of c-ZrO_2 with respect to the total ZrO_2 at 1400 °C (obtained using Garvie and Nicholson method) was nearly 20 and 40% for 5 and 15 mol% CaO, respectively, and then reached 76% at 30 mol%. For 50 mol% the ZrO_2 stabilization was nearly complete (94%). Thus, high CaO to ZrO_2 ratio enhanced the m → c phase transformation.

3.2. Sintering and textural characteristics

Figs. 3 and 4 show the effect of the content of CaO in the starting composition on open pore size distribution and mean pore radius of ceramics sintered at 1400 °C. The samples had a monomodal pore size distribution which was composed by

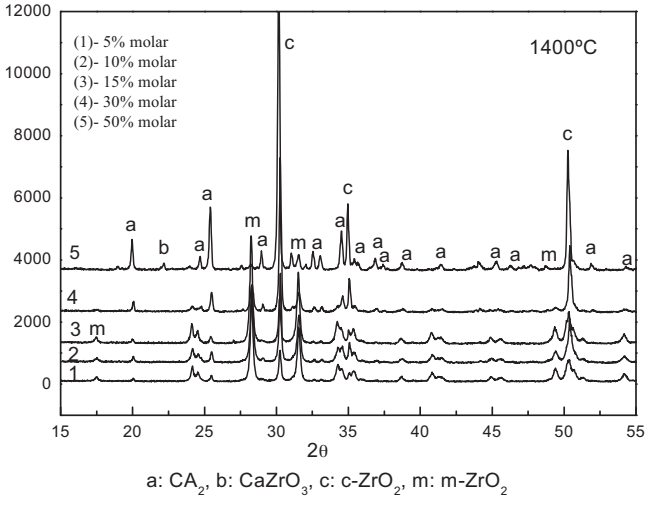

Fig. 1. XRD patterns of ceramics with 5–50 mol% CaO in ZrO_2 and sintered at 1400 °C.

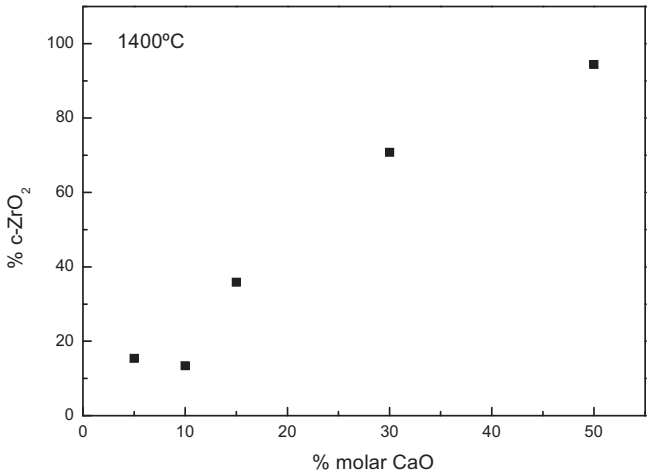

Fig. 2. Relative content of c-ZrO_2 vs. mol% CaO.

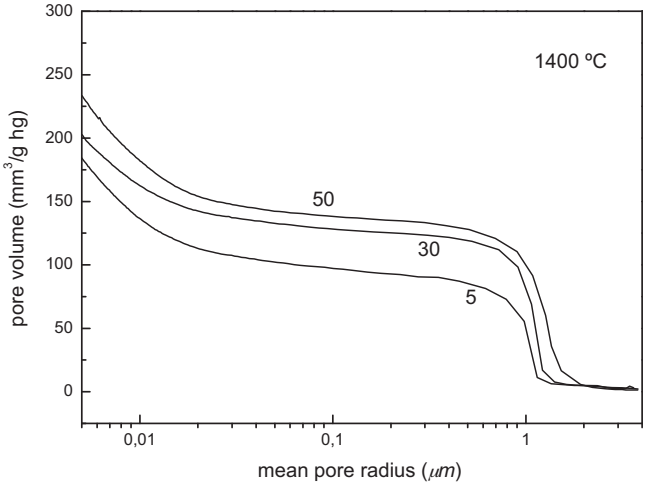

Fig. 3. Cumulative pore size distribution curves of composites sintered at 1400 °C for different CaO content.

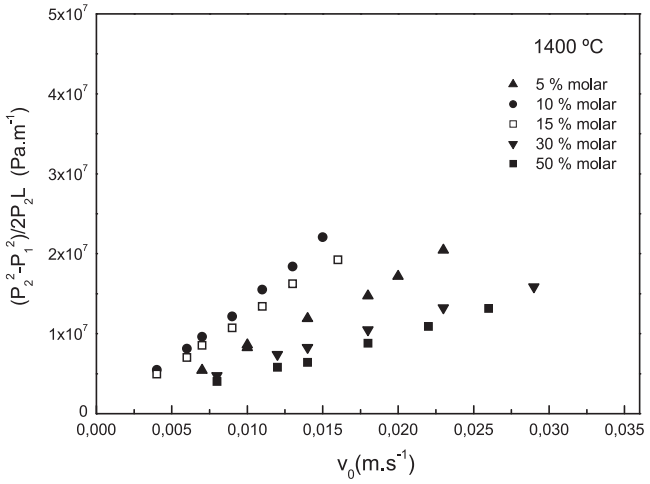

Fig. 5. Pressure drop vs. velocity curves for composites with 5–50 mol% of CaO sintered at 1400 °C.

pores having the characteristic radius near to 1 μm. High CaO concentration shifted the maximum of pore size distribution to higher radius from 1.1 to 1.3 μm. Moreover, according to the respective cumulative curves, a fine population of pores with radius <0.01 μm existed which probably originated by the intra-aggregated pores (i.e. interstices between primary zirconia particles). The relative volume fraction of the smallest detectable pores remained close to 0.3 for the different compositions studied. In particular, the composite containing 50 mol% CaO exhibited a wider pore size distribution for which the coarser fraction with pore radius above 1.5 μm notably increased. Also the maximum intruded volume of Hg increased with increasing CaO.

3.3. Effect of composition on experimental permeability

The pressure drop through the porous composite vs. gas velocity curves of sintered composites produced from different compositions (Fig. 5) were used to determine the permeability constants k_1 an k_2 by fitting with the Forchheimer model (Eq. (1)). Table 2 shows that both constants of the ceramic disks increased with % molar of CaO in the different compositions. This result can be clearly observed in Fig. 5 as the slopes of the lines are inversely proportional to the permeability constant (Eq. (1)).

The k_1 and k_2 data obtained in this work varied between 2.2–3.6 × 10^{-14} m^2, for k_1 and 9.8–7.2 × 10^{-10} for k_2 which are in the same order of magnitude with those permeability constants previously reported for porous structures of mullite-alumina produced by slip casting with 50 vol% porosity and micrometer pore diameters of 1–4 μm [19].

The similar pressure drop curves as that of Fig. 5 were found for samples sintered at different temperatures. Most of composites followed the same linear relationship between pressure drop and velocity showing an increase in the slope from 1300 to 1450 °C (i.e. a reduction in permeability). Contrarily, the sample containing 50 mol% CaO (Fig. 6) showed an inverse tendency but in agreement with a linear behavior of the pressure drop.

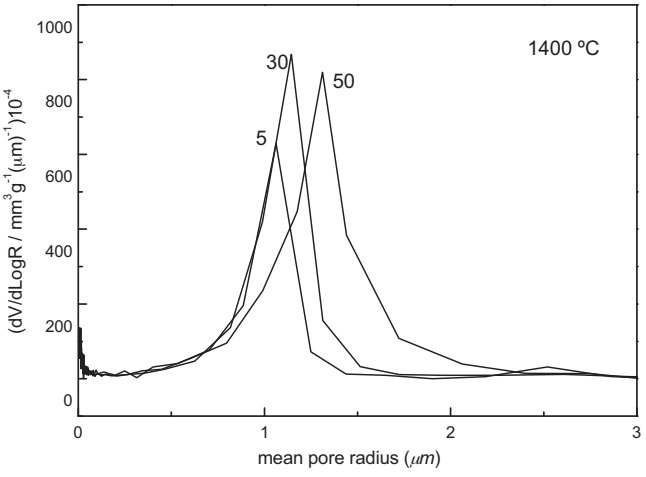

Fig. 4. Differential pore size distribution curves of composites sintered at 1400 °C for different CaO content.

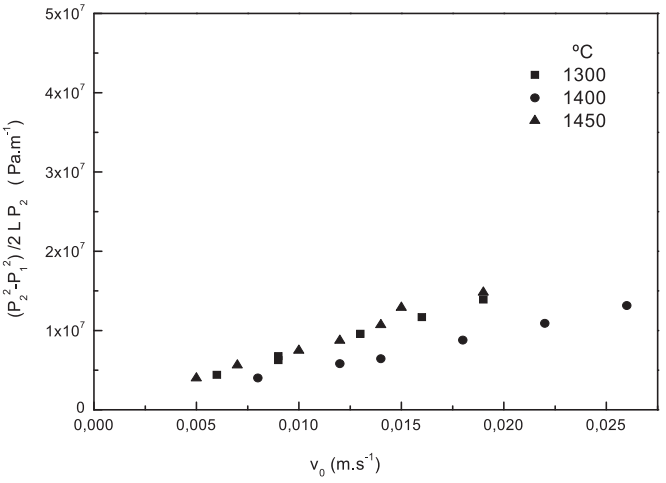

Fig. 6. Pressure drop vs. velocity curves of composites with 50 mol% of CaO sintered at 1300–1450 °C.

Table 2
Permeability of porous composites evaluated using Forchheimer and Darcy models for different contents of CaO in the starting composition.

mol%	Darcy	Forchheimer				
	k_1 (m^2)	k_1 (m^2)	k_2 (m)	k_1/k_2	F_0	Deviation (%)
5	2.20E−14	2.14E−14	7.18E−10	2.98E−05	0.027	2.67
15	1.30E−14	1.49E−14	2.99E−10	4.97E−05	0.03	2.92
30	3.06E−14	3.34E−14	9.28E−10	3.60E−05	0.045	4.27
50	3.63E−14	3.31E−14	9.8E −10	3.38E−05	0.041	3.92

Furthermore, the linear relation between pressure drop and velocity of Figs. 5 and 6 suggested that the inertial and turbulent effects (the quadratic term of Eq. (1)) can be neglected. To confirm this result, experimental data were also fitted with Darcy's equation. The resultant parameter k_1 and the corresponding deviation (which was calculated using Eq. (6)) are included in Table 2.

According to Table 2 the Darcian permeability k_1 resulted close to $2–4 \times 10^{-14}\ m^2$ and the calculation using the parameter F_0 indicated that the contribution of viscous forces approximated to 95% of the total pressure gradient for the low range of velocities 0.05–0.35 m s^{-1}. The minor deviations obtained using the Darcy model (Table 2) confirmed that the k_1 was representative of the permeability of the porous composites.

The relation between Darcian k_1 and non Darcian k_2 permeability obtained in this work agreed well with that expected for sintered ceramics included in a data map available in the literature for several types of porous structures [18]. Therefore a change of porous microstructure should produce more significant variation in k_2 than in k_1. Thus in a case of a flow regime with a high gas velocity range (i.e. Reynolds numbers > 10), the k_2 would not be neglected because is expected a significant increase in the parameter F_0.

In this study, permeability k_1 increased with increasing pore volume and mean size as is shown in Fig. 4.

3.4. Effect of composition on microstructure

SEM micrographs of Figs. 7 and 8 show a typical agglomerated microstructures of composites, the aggregates present in the starting ZrO_2 powder remained in the sintered composite. Light and gray color areas that appeared in the complex microstructure correspond to ZrO_2 and CA_2 phases, respectively. Composites contained significant amount of pores (in dark color) as sintering of highly aggregated powder provided a highly porous ceramic. Pores were present as

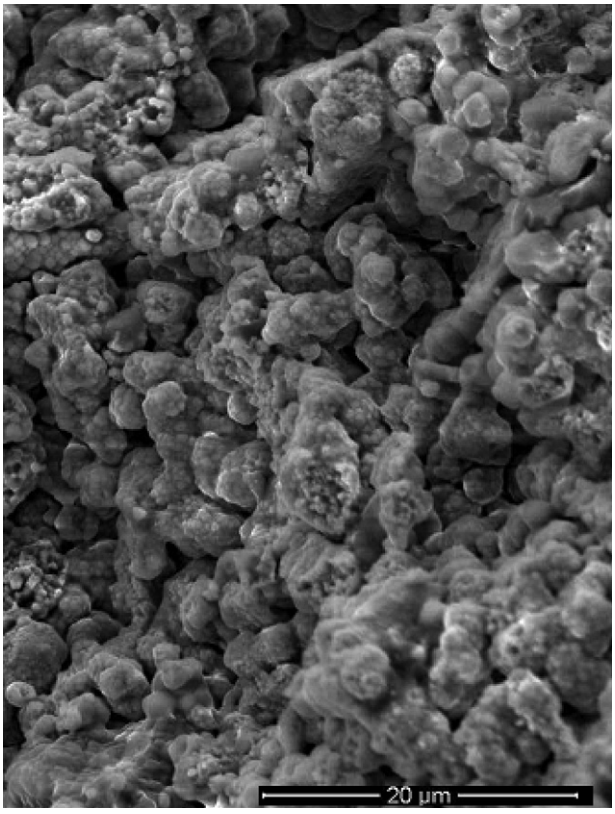

Fig. 7. SEM micrograph of fracture surface of composites with 5 mol% of CaO.

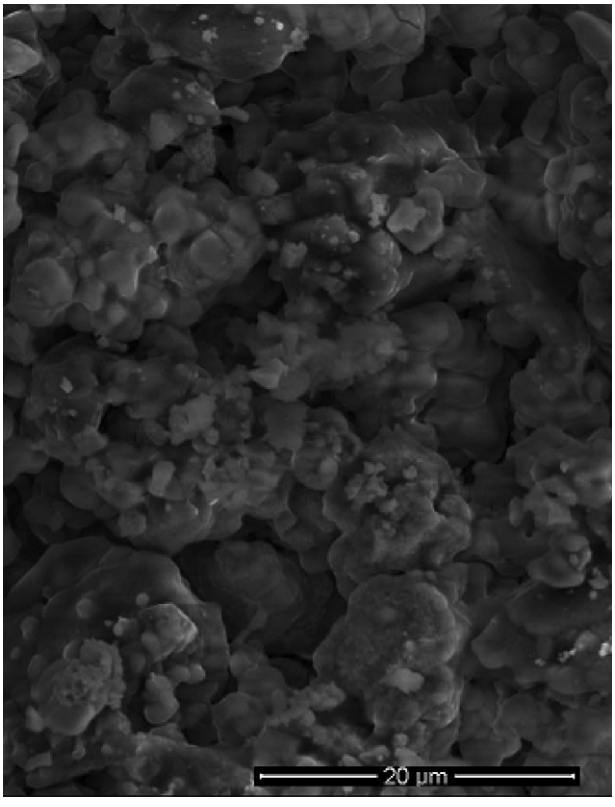

Fig. 8. SEM micrograph of fracture surface of composites with 30 mol% of CaO.

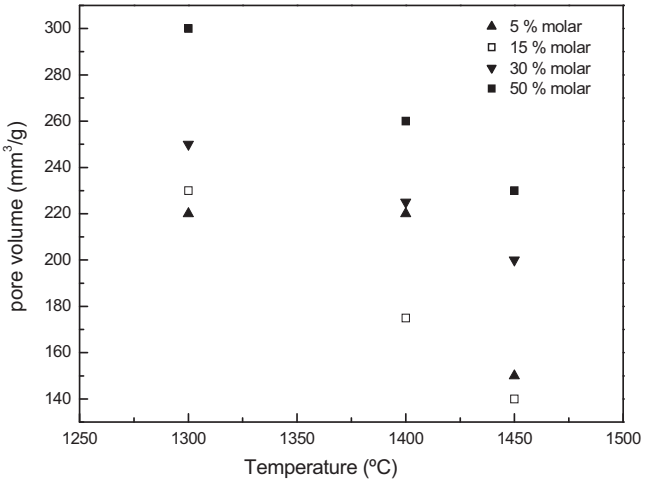

Fig. 9. Pore volume vs. sintering temperature for composites with 5, 15, 30 and 50 mol% of CaO.

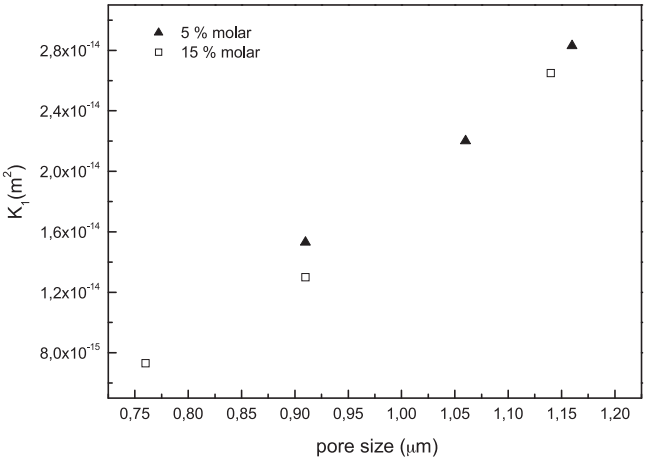

Fig. 11. Permeability vs. mean pore size for composites with 5, 15, 30 and 50 mol% of CaO sintered at different temperatures.

interparticle voids and channels in agreement with the processing method used. Porous structure consisted of irregular shaped pores with a range of sizes. Relatively large pore size was obtained with the 30 mol% of CaO addition. Also a continuous phase gradually appeared with increasing CaO content (gray color) and it was observed surrounding the zirconia aggregates. Therefore, the increase in the porosity and pore size observed for high CaO contents close to 50 mol% was mainly related to both the low relative zirconia content and the probable existence of liquid phase that accelerated the pore growing from the coalescence of the low sized pores.

3.5. Effect of sintering temperature on structure parameters and correlation with experimental Darcian permeability

Permeability is mainly dependent on structural parameters like morphology, size, volume of pores as well as type of porous structure.

The effect of the sintering temperature on textural properties of the composites containing 5, 15, 30 and 50 mol% CaO and the correlation with permeability was examined. Figs. 9 and 10 show the variation of pore volume and mean pore size with sintering temperature for all samples.

Fig. 9 shows that the maximum Hg intruded volume decreased with the sintering temperature for composites containing 5 and 50 mol% CaO. Moreover, resultant pore volume increased with increasing CaO addition. Thus, porosity of ceramic with 50 mol% CaO reduced from 300 at 1300 °C to 230 Hg mm^3/g at 1450 °C. For this material, Fig. 10 shows that the most frequent pore radius increased from 1.25 to 1.53 μm after sintering at 1300 and 1450 °C, respectively. A similar effect was observed for the composites containing 30 mol% CaO. Contrarily, the ceramics containing 5 and 15 mol% CaO showed that in both cases the pore size decreased with the sintering temperature as sintering progressed.

Figs. 11 and 12 show that the experimental Darcian permeability k_1 varied between 2.2 and 3.6×10^{-14} m^2 for 1300 to 1450 °C. For composites produced from low CaO

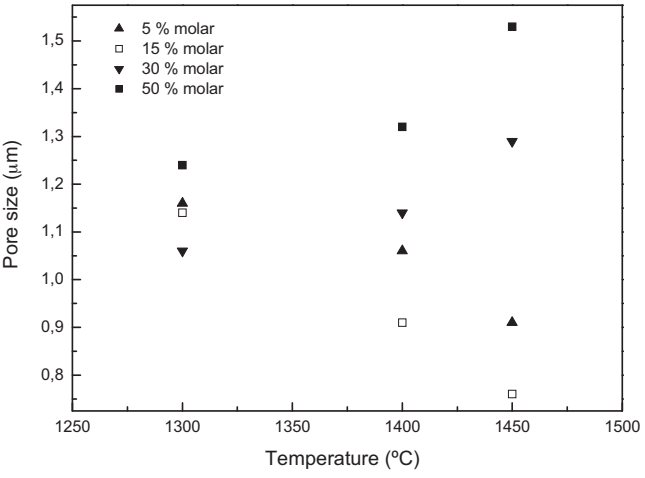

Fig. 10. Pore size vs. sintering temperature for composites with 5, 15, 30 and 50 mol% of CaO.

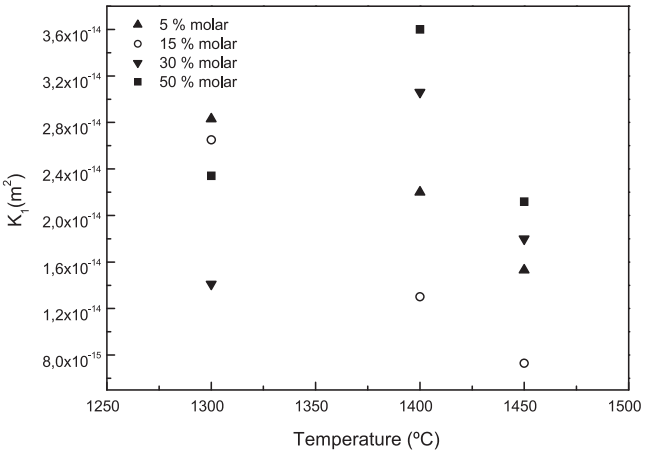

Fig. 12. Permeability vs. sintering temperature for composites with 5, 15, 30 and 50 mol% of CaO.

addition the small reduction in k_1 with sintering temperature may be explained by the relatively low open porosity and pore size, as determined by Hg porosimetry, at high temperatures. Whereas the k_1 remained nearly constant for the composite with 50 mol% CaO by sintering up to 1450 °C probably due to combined effect of the reduction in pore volume and the slightly higher mean pore size with respect to those of 1300 °C.

In summary, we observed for all composites that pore volume decreased with temperature. However, Fig. 10 shows that there was no direct function between the pore radius and temperature. Nevertheless, Fig. 12 indicates that permeability of most of the composited containing low CaO decreased with temperature. The deviation to this trend was observed for the cases where the pore radius increased with temperature. This is because permeability is a nonlinear function of pore volume and pore radius (as reflected in the Ergun equation), which also explains the case of the two different permeability values for a constant pore volume.

3.6. Theoretical prediction of permeability k_1

Fig. 13 shows the comparison between permeability k_1 derived from Ergun's equations [Eqs. (3) and (4)] and permeability constants obtained experimentally.

The permeability constants k_1 obtained from Ergun's equation was calculated using the textural parameters obtained by Hg porosimetry and were found in values ranging between 3.2 and 4.1×10^{-14} m^2, being slightly higher than those measured experimentally.

The deviation between experimental and predicted k_1 increased with N_2 velocity, and varied between 12 and 31%. High deviation indicated that hydraulic radius was not appropriate as a parameter for describing the characteristic length of the porous medium.

That is, the real porous medium (consisting in a random packing of solid particles) developed interconnected pores without a definite pore shape and size which are not accounted for the idealized geometry assumed in the Ergun's model (parallel channels of cylindrical geometry). The porous microstructure

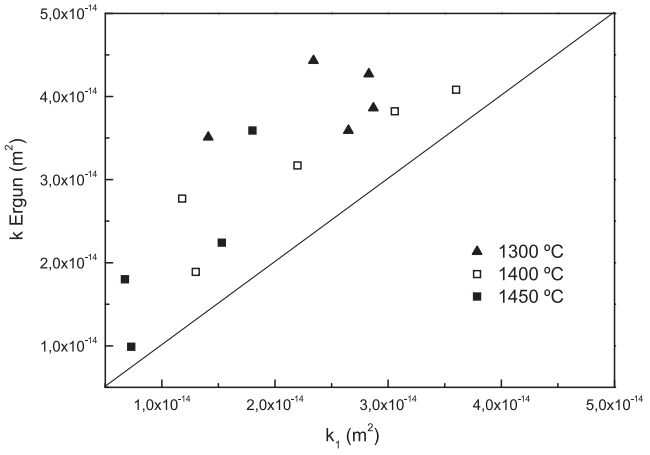

Fig. 13. Comparison between experimental permeability and theoretical values estimated using the Ergun's equation.

results sensitive to change as the sintering progresses. Therefore, the actual length of fluid path is longer than the characteristic length used as representative. For this reason it is extremely difficult to find an effective model that describes the relationship between permeability as a function of simple structure parameters like porosity and particle size and/or the mean size of voids that form the pore space. Nevertheless, the Ergun's equation provided a reasonable estimation of the permeability (the same order of magnitude) in a range of those N_2 velocities studied in this work (laminar regimes Reynolds number $Re < 1$) for porous granular composites with micrometer sized pores.

4. Conclusions

Formation of Ca stabilized ZrO_2 in mixtures containing pure ZrO_2 and calcium aluminate cement (5–50 mol% CaO in ZrO_2) was achieved between 1300 and 1450 °C. For all compositions, porous composites can be effectively produced by dry pressing and reaction sintering at 1300–1450 °C without any visible cracks.

The ceramic with low CaO addition after sintering at 1400 °C was predominantly composed by m-ZrO_2 and a cubic zirconia solid solution (c-ZrO_2; $Ca_{0.15}Zr_{0.85}O_{1.85}$) with residual CA_2. In this case, probably t-ZrO_2 and c-ZrO_2 coexisted. With increasing the CaO amount to 30 and 50 mol% and the sintering temperature, the main constituents were c-ZrO_2 and CA_2 with $CaZrO_3$ as a secondary phase and CA as impurity. Scarce $CaZrO_3$ was detected for 30 mol% CaO in the composition, and its amount slightly increased for 50 mol% CaO.

Forchheimer and Darcy's models fitted well the experimental data of pressure drop vs. N_2 velocity. The viscous forces contributed to near 95% of the total pressure gradient and therefore the inertial forces could be neglected in the low velocities range studied. Darcian permeability k_1 varied between 2 and 4×10^{-14} m^2 and was found representative of the gas transport flow through the porous composites.

Most composites showed a monomodal pore size distribution with a typical pore size of 1–1.3 μm. In addition, composites with 30 and 50 mol% of CaO showed a gradual increase in both pore volume and volume fraction of pores having radius in a range of 1.5–2 μm. Thus, high CaO concentration in the composition enhanced k_1 while the increase in sintering temperature reduced the N_2 flow. Similar permeability k_1 of composites with 50 mol% CaO sintered at 1300–1450 °C may be explained by a combined effect of relatively low pore volume and high pore size.

Ergun's equation overestimated the N_2 permeability constant with respect to that obtained experimentally. This limitation was attributed to the actual length path of the gas that is greater than the idealized length defined by that model. Nevertheless, this model provided a correct trend of k_1 with increasing CaO.

References

[1] B. Basu, Toughening of yttria-stabilised tetragonal zirconia ceramics, Int. Mater. Rev. 50 (4) (2005) 239–256.
[2] P. Shuk, E. Bailey, U. Guth, Zirconia oxygen sensor for the process application: state-of-the-art, Sens. Transducers J. 90 (2008) 174–184.

[3] J.-H. Lee, Review on zirconia air-fuel ratio sensors for automotive applications, J. Mater. Sci. 38 (2003) 4247–4257.
[4] C. Piconi, G.A. Maccauro, Zirconia as a ceramic biomaterial, Biomaterials 20 (1) (1999) 1–25.
[5] Y. Zhao, W. Li, M. Zhang, K. Tao, A comparison of surface acidic features between tetragonal and monoclinic nanostructured zirconia, Catal. Commun. 3 (6) (2002) 239–245.
[6] A. Larbot, J-P. Fabre, Ch. Guizard, L. Cot, New inorganic ultrafiltration membranes: titania and zirconia membranes, J. Am. Ceram. Soc. 72 (1989) 257–261.
[7] S. Nath, N. Sinha, B. Basu, Microstructure, mechanical and tribological properties of microwave sintered calcia-doped zirconia for biomedical applications, Ceram. Int. 34 (2008) 1509–1520.
[8] S.K. Durrani, J. Akhtar, M. Ahmad, M.A. Hussain, Synthesis and characterization of low density calcia stabilized zirconia ceramic for high temperature furnace application, Mater. Chem. Phys. 100 (2006) 324–328.
[9] F. Shojai, T. Mantyla, Monoclinic zirconia microfiltration membranes: preparation and characterization, J. Porous Mater. 8 (2001) 129–142.
[10] J. Zhang, F. Ye, J. Sun, D. Jiang, M. Iwasa, Aqueous processing of fine ZrO_2 particles, Colloids Surf. A: Physicochem. Eng. Aspects 254 (2005) 199–205.
[11] K.M. Parker, J.H. Sharp, Refractory calcium aluminate cements, Trans. J. Br. Ceram. Soc. 81 (1982) 35–42.
[12] T. Isobe, Y. Kameshima, A. Nakajima, K. Okada, Y. Hotta, Gas permeability and mechanical properties of porous alumina ceramics with unidirectionally aligned pores, J. Eur. Ceram. Soc. 27 (2007) 53–59.
[13] W.L. Vasconcelos, Description of permeability in porous ceramics, Cerâmica 43 (1997) 281–282.
[14] E.A. Moreira, M.D.M. Innocentini, J.R. Coury, Permeability of ceramic foams to compressible and incompressible flow, J. Eur. Ceram. Soc. 24 (2004) 3209–3218.
[15] M.D.M. Innocentini, V.R. Salvini, A. Macedo, V.C. Pandolfelli, Prediction of ceramic foams permeability using Ergun's equation, Mater. Res. 2 (1999) 283–289.
[16] M.D.M. Innocentini, V.R. Salvini, V.C. Pandolfelli, J.R. Coury, Assessment of Forchheimer's equation to predict the permeability of ceramic foams, J. Am. Ceram. Soc. 82 (1999) 1945–1948.
[17] F.S. Ortega, F.A.O. Valenzuela, C.H. Scuracchio, V.C. Pandolfelli, Alternative gelling agents for the gelcasting of ceramic foams, J. Eur. Ceram. Soc. 23 (2003) 75–80.
[18] M.D.M. Innocentini, R.K. Faleiros, R. Pisani Jr., I. Thijs, J. Luyten, S. Mullens, Permeability of porous gelcast scaffolds for bone tissue engineering, J. Porous Mater. 17 (2010) 615–627.
[19] L.F. Berti, P.H.D. Santos, E. Bazzo, R. Janssen, D. Hotza, C.R. Rambo, Evaluation of permeability of ceramic wick structures for two phase heat transfer devices, Appl. Therm. Eng. 31 (2011) 1076–1081.
[20] R.B. Bird, W.E. Stewart, E.N. Lightfoot, Fenómenos de transporte, Reverté, Barcelona, 1973.
[21] R. Garvie, P.S. Nicholson, Phase analysis in zirconia systems, J. Am. Ceram. Soc. 55 (1972) 303–305.
[22] C. Clar, A.N. Scian, E.F. Aglietti, Estudio del Envejecimiento del Gel de Acetato Básico de Aluminio y su Influencia en la Permeabilidad de las Membranas Obtenidas, Rev. Matér. 10 (2005) 185–191.
[23] T. Muromura, Y. Hinatsu, Phase relation of ternary system ZrO_2–CaO–Al_2O_3, Mater. Res. Bull. 21 (1986) 61–67.
[24] J. Bu, P. Wang, L. Ai, X. Sang, Y. Li, Research on the technical conditions on synthesizing calcium zirconate material, Adv. Mater. Res. 287–290 (2011) 1765–1770.